

# Damage detection in hybrid metal-composite plates using ultrasonic guided waves based on outliers estimate

Faez Masurkar<sup>1,a,\*</sup>, Fangsen Cui<sup>1,b</sup>

<sup>1</sup>Institute of High Performance Computing (IHPC), Agency for Science, Technology, and Research (A\*STAR), Singapore 138632

<sup>a</sup>Masurkar\_Faez\_Aziz@ihpc.a-star.edu.sg, <sup>b</sup>cui@ihpc.a-star.edu.sg

**Keywords:** Hybrid Metal-Composite Plates, Ultrasonic Guided Waves, Feature Extraction, Data-Driven Damage Detection, Outlier Detection

**Abstract.** The present research focusses on the development of a robust data-driven damage diagnosis technique to detect different types of damages in a hybrid metal-composite (HMC) plate specimen resulting from manufacturing processes, loading conditions, and ambient environmental conditions. These defects over a course of time deteriorate the load-bearing capacity of the HMC's and in turn, their reliability in terms of safe operation. In this work, ultrasonic guided waves (UGW) are used for non-destructive evaluation (NDE) of the HMC. The use of UGW for NDE offers advantages such as long-range inspection and sensitivity to small-sized surface and sub-surface damages. The ultrasonic tests are simulated using a pitch-catch active sensing technique at a typical frequency-mode pair best suited to detect and classify damages in the HMCs. The damage-sensitive feature is extracted from the received UGW using Hilbert transform-based feature extraction method. The damage indicator is classified in the damage-sensitive feature space using the root mean square technique identified as outliers, which is further used to classify the detected damages. The achieved results manifest the ability of the proposed technique to be a part of the industrial structural integrity inspection process typically for HMCs in detecting and classifying embedded damages with high accuracy.

## Introduction

Composite materials are widely used in the aerospace industry, with nearly 80% of structural volume of an aircraft, due to their high fatigue strength, low density, and corrosion resistance. Unlike metals, damage in composites appears prematurely, but propagates in a more stable way. Thus, they have an upper end compared to metals particularly when subjected to fatigue loading primarily because of the complicated relationship between the fibers, matrix, damage, and the residual stresses that block the propagation of damage [1]. In the case of fiber re-enforced composites, defects can occur in the matrix, fiber, or at the interface. The major defects are the delamination, debonding in the fiber matrix interface, waviness, fiber breakage, matrix cracking, porosity etc. Further, if the layered composite is attached to a metal plate, resulting in a Hybrid metal composite assembly, disbond damage can occur between the metal-composite interface.

Guided waves are of paramount importance for non-destructive testing (NDT) of engineering structures such as rail tracks, pipes used to transport oil and gas, nuclear reactors, adhesive bonds, aircraft components, civil structures, and many more. These waves travel sufficiently longer distances and can capture any potential irregularities of the propagating medium. However, these waves are multimodal and highly dispersive. Thus, a careful selection of the frequency-mode pair is essential to ensure effective inspection of the structure [2-3].

Lugovtsova et.al [4] studied propagation of guided waves in a multi-layered CFRP-Aluminum structure to detect cracks and delamination. Yan et.al. [5] studied the interaction of ultrasonic guided waves and delamination in a 23-layer Alcoa Advanced Hybrid Structural plate. Papanaboina et.al [6] focused on the numerical analysis of the guided waves propagation in a

multilayered CFRP structure to refine damage detection and its localization using different signal processing methods. Zhang et.al. and Liu et.al. [7-8] studied the defect and waviness detection in a layered composite using ultrasound.

The present study focusses on the NDT of a HMC specimen using ultrasonic guided waves. Firstly, a suitable frequency-mode pair was identified through the dispersion diagram best suited to detect disbond and delamination damage in the specimen. Next, this frequency-mode pair was excited using a wedge transducer and multiple responses were recorded along the wave propagation direction. The received time-domain responses were analyzed using the Hilbert-Huang transform (HHT) and the Hilbert envelopes and phases were evaluated. Lastly, a classification of damages was performed based on the outliers estimated using the RMS of Hilbert phases. Finally, findings from the present study were summarized.

### Methodology

The present study focusses on the damage detection in a HMC specimen using a typical ultrasonic guided wave mode. For this purpose, signal processing of the received ultrasonic signals is conducted using the Hilbert-Huang transform algorithm to extract the Hilbert envelope and the phase. The envelope can be useful for estimating the arrival time of incident wave packet and damage reflected wave packet which can be eventually used for damage detection and localization; whereas the Hilbert phase is useful to classify the detected damage. The following sub-section presents the background of the HHT algorithm.

#### The Hilbert-Huang transform algorithm:

The HHT is a method to decompose the time-transient signal into intrinsic mode functions (IMFs) and estimate instantaneous phase or frequency. These IMFs can be regarded as a basis of expansion which can linear or nonlinear in nature. An instantaneous phase ( $\phi(t)$ ) can be defined by an analytical signal as [9]:

$$y(t) = x(t) + iH[x(t)] = a(t)e^{i\phi(t)}, \quad (1)$$

where 'x(t)' is the time-domain signal and the imaginary part is the Hilbert transform of 'x(t)', further  $a(t) = \sqrt{[x(t)]^2 + \{H[x(t)]\}^2}$ , and  $\phi(t) = \arctan \{H[x(t)]/x(t)\}$ . The total instantaneous phase is calculated as the sum of the instantaneous phases of each IMF's given as:

$$\phi(t) = \sum_{i=1}^n \arctan \left\{ \frac{H[x_i(t)]}{x_i(t)} \right\} \quad (2)$$

Due to the properties of the IMF's the Hilbert phase monotonically increases with time.

### Numerical study

In the present study, the ultrasonic guided waves are excited and sensed using a wedge transducer and the guided wave responses are recorded in a pitch catch configuration. This ensures that a desired guided wave mode is actuated and sensed through the Finite Element (FE) model setup [10-11]. The materials used in the simulation and their mechanical properties are presented in the following subsection.

#### Material description and defects:

The specimen used for the present study is a HMC specimen that comprises of two metal plates affixed to composite plies as shown in Fig.1. The metal plate is an Al 6061 specimen whereas the composite plies are made of Uni-directional carbon fiber laminates (U-CFL) stacked on top of each other with stacking sequence  $[0/+45/-45/90]_{2s}$ . As shown schematically in Fig.1, there are two plates of Aluminum and 16 plies of U-CFL. The material properties of metal and composite

are given in Table 1 and Table 2 respectively. Further, the mechanical properties of the wedge material are also given in Table 1.

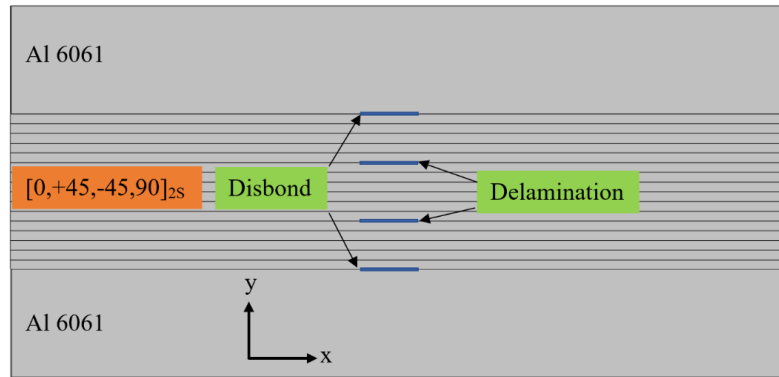


Fig.1. Schematic of the HMC specimen showing Al and U-CFL material along with defects.

Table 1 Mechanical properties of Al 6061 and PMMA wedge

| Material | Thickness (mm) | $\rho$ (Kg/m <sup>3</sup> ) | E(GPa) | $\nu$ [-] | $V_L$ (m/s) | $V_T$ (m/s) |
|----------|----------------|-----------------------------|--------|-----------|-------------|-------------|
| Al6061   | 1.6            | 2700                        | 68.9   | 0.33      | 6148.9      | 3097.3      |
| PMMA     | -              | 1185                        | 2.3    | 0.35      | 1765        | 847.9       |

Table 2 Mechanical properties of U-CFL [0<sup>0</sup>]

| Thickness (mm) | $C_{11}$ (GPa) | $C_{12}, C_{13}$ (GPa) | $C_{22}$ (GPa) | $C_{23}$ (GPa) | $C_{33}$ (GPa) | $C_{44}$ (GPa) | $C_{55}, C_{66}$ (GPa) | $\rho$ kg/m <sup>3</sup> |
|----------------|----------------|------------------------|----------------|----------------|----------------|----------------|------------------------|--------------------------|
| 0.25           | 165.24         | 6.63                   | 14.32          | 6.39           | 14.32          | 3.96           | 5.17                   | 1560                     |

Two different types of defects are considered in the present study namely delamination and disbond. Delamination is a type of defect that occurs between neighbouring plies whereas disbond is a defect that occurs between a metal and composite ply layer.

**Dispersion curves & wave structures of the HMC specimen:**

The structural integrity of the HMC specimen is evaluated using ultrasonic guided waves in contrast to the conventional bulk wave-based C-Scan technique. However, to apply a guided wave-based defect detection strategy in a HMC specimen, it is paramount to firstly obtain the guided wave dispersion curves that describes all the possible mode-frequencies which are available for structural integrity inspection. Further analysis of the dispersion curves shall reveal the most sensitive modes that can provide inspection of the specimen not only near to specimen surface but also across whole of its thickness. This is the primary reason of selecting guided wave-based inspection technology in contrast to the conventional bulk wave C-Scan technique. The dispersion curves obtained for a HMC specimen are shown in Fig.2. To select a suitable wave mode for damage inspection, wave structures of each Lamb mode are studied at different frequencies, and it is found that the  $A_1$  Lamb mode at 500 kHz excitation frequency is suitable for damage inspection in the considered HMC specimen as shown in an inset diagram in Fig.2. Thus, the excitation frequency is selected as 15.5 cycles gaussian modulated sine wave signal that is centered at 500 kHz. This time-domain excitation signal and its frequency spectrum is shown in Fig.3.

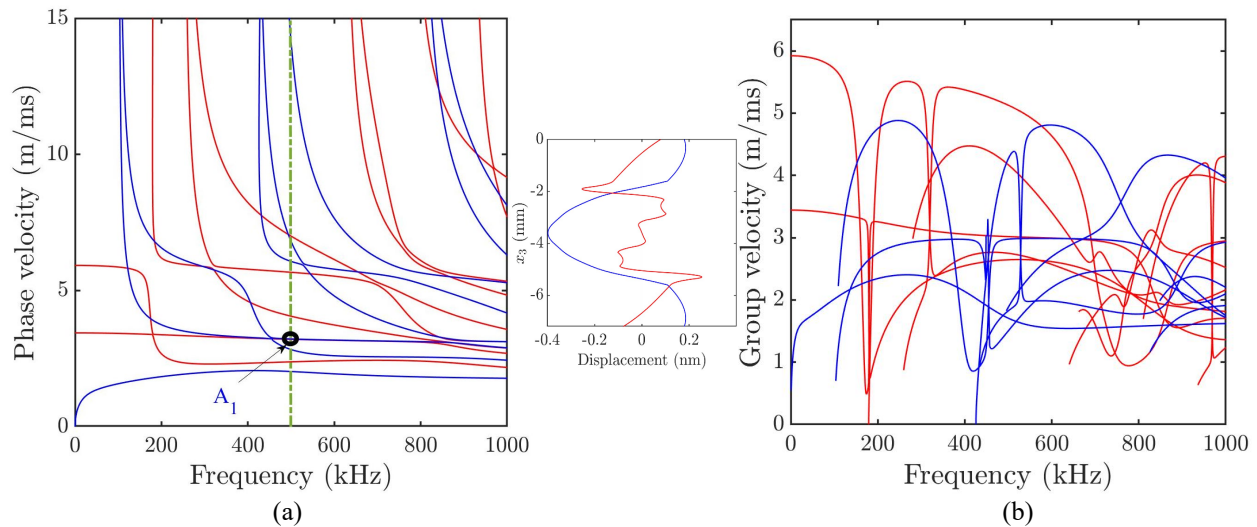


Fig.2 Dispersion Curves of HMC specimen (a) Phase velocity (b) Group velocity.

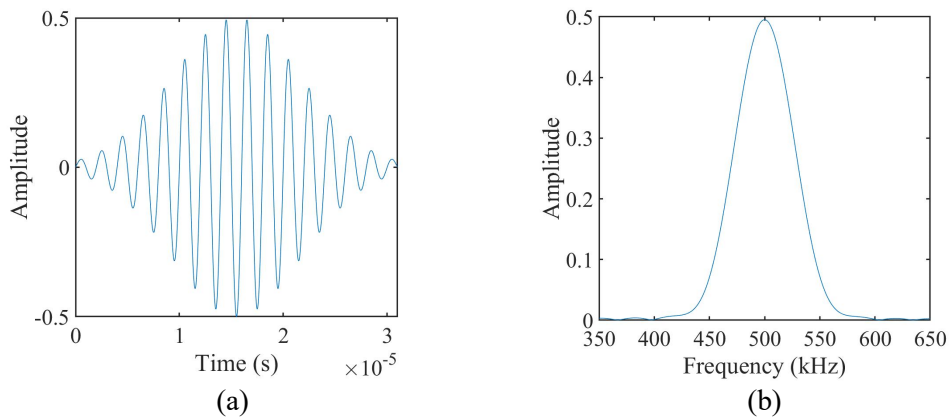


Fig.3 The excitation signal used in FE simulations (a) Time domain (b) Frequency domain.

### Finite Element model

In the present study, the guided wave responses were excited using a wedge transducer affixed on top of the HMC specimen and sensed along different receiving points on plate surface as shown schematically in Fig.4. A normal transducer attached to the PMMA wedge is modelled to simulate a wedge transducer that act as an actuator and generates a desired guided wave mode in the HMC test specimen. The angle of excitation or the wedge angle is estimated using the Snell’s law as shown in Eq.3. On the receiver side, in-plane and out-of-plane time domain responses are recorded on the HMC specimen surface with a uniform incremental steps of 10 mm.

$$\theta_{A_1} = \sin^{-1} \left( \frac{V_{L|Wedge}}{V_{A_1|Plate}} \right) \quad (3)$$

Further absorbing boundary conditions are enforced at the start and end of the HMC plate across thickness direction as well as along all edges of wedge except the excitation edge and wedge-HMC interface as shown in Fig.4.

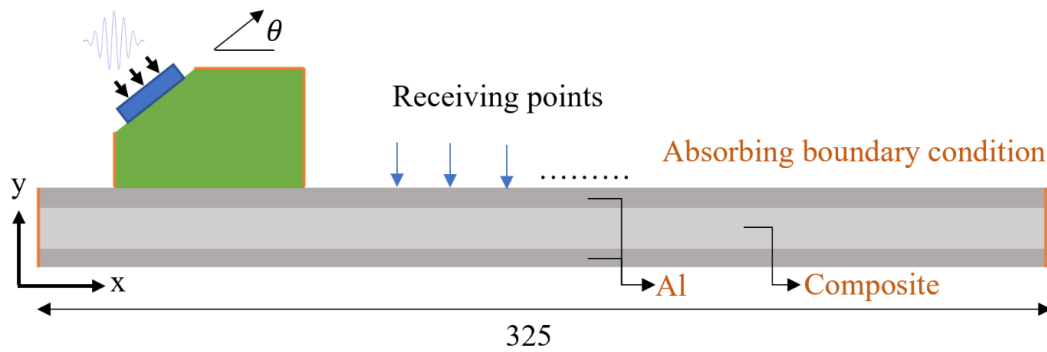


Fig.4 Schematic of the 2D FE model (All dimensions are in mm).

**Results and discussions**

The results of FE simulations conducted at 500 kHz for an intact HMC specimen is presented firstly in this section. The wave propagation in the wedge-HMC assembly for an intact specimen is shown in Fig.5. The longitudinal wave excited at the flank of the wedge is converted to  $A_1$  Lamb mode at a critical angle of  $33.23^\circ$ . Further, time-domain waveforms at the intact condition of the specimen are presented in Fig.6 for in-plane and out-of-plane motion. It shows a pure generation of  $A_1$  Lamb mode with no potential reflections from damage.

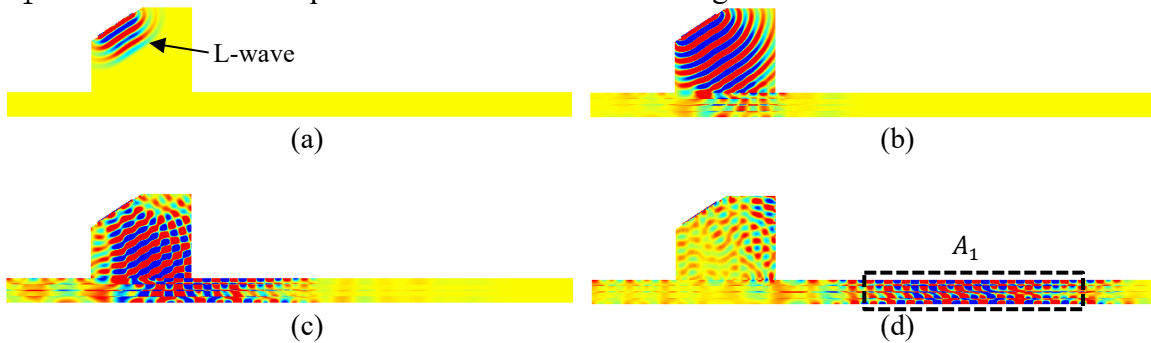


Fig.5 Wave propagation at different time instants in a intact HMC specimen.

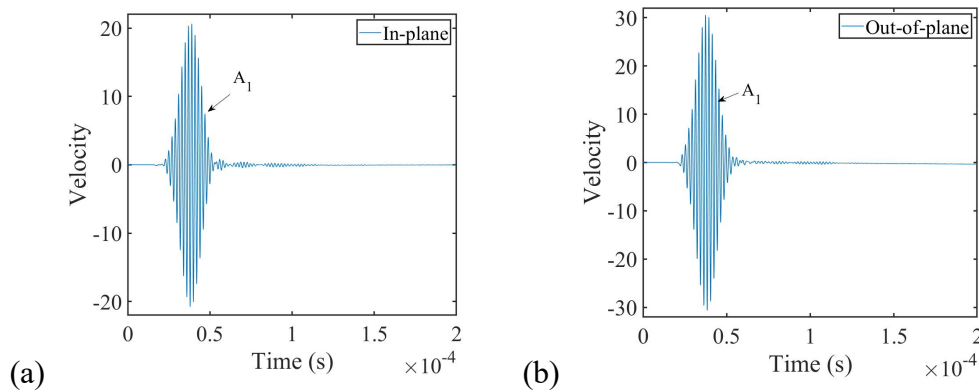


Fig.6 Time domain waveforms for a healthy HMC specimen at (70,7.2) mm from origin.

Further, a disbond damage was created in the specimen model centered (155, 5.65) mm from the origin. The time domain signals received at 70 mm and 100 mm are shown in Fig.7 and Fig.8 respectively. It can be clearly seen in Fig.7; an additional wave packet being reflected from the disbond damage. It is also observed from Fig.8, when the sensing point is far away from damage, the out-of-plane motion captures smaller wave packets that are reflected from the front and back edge of the disbond. However, when the sensing point moves closer to the damage, these two

smaller wave packets merge into one bigger wave packet, as a result of reduced wave propagation distance from damage to sensing point as shown in Fig.8.

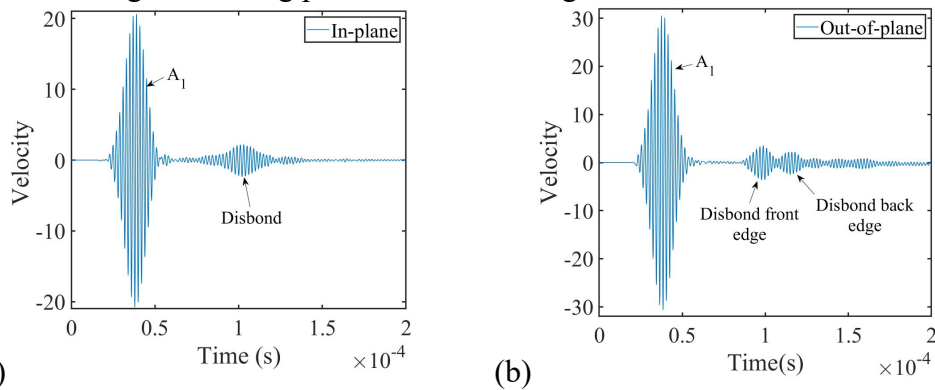


Fig.7 Time domain waveforms for a HMC specimen with disbond at (70,7.2) mm from origin.

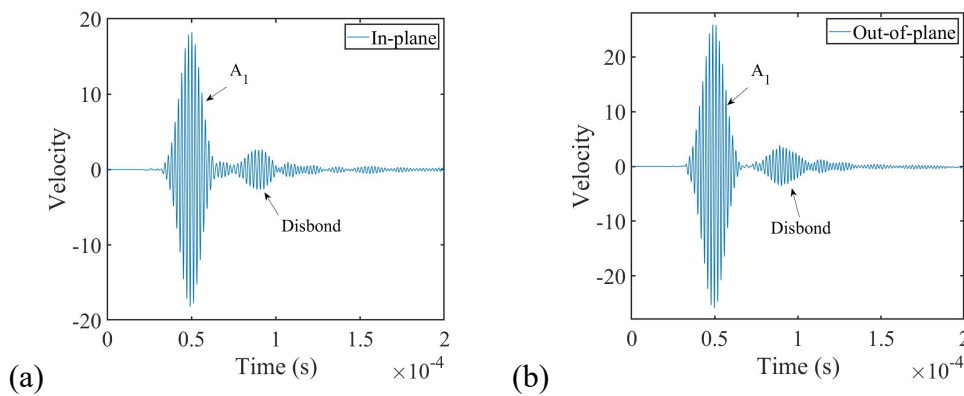


Fig.8 Time domain waveforms for a HMC specimen with disbond at (100,7.2) mm from origin.

Next, delamination damage was created in the specimen model centered (155, 4.35) mm from the origin. The time domain signals received at 70 mm & 100 mm are shown in Fig.9 and Fig.10 respectively. Similarly, additional wave packets reflected from the delamination damage were observed. The Hilbert envelope and phases were evaluated for healthy and damaged HMC specimens as shown in Fig.11(a)-(c). The envelope for a disbond damage was seen to have significant deviation from healthy specimen compared to delamination damage which was also seen in the Hilbert phase. In order to facilitate classification, RMS of the Hilbert phase was evaluated and shown in Fig.11 (d). The disbond damage exhibit maximum RMS whereas the delamination damage has intermediate value and lastly followed by the healthy HMC specimen.

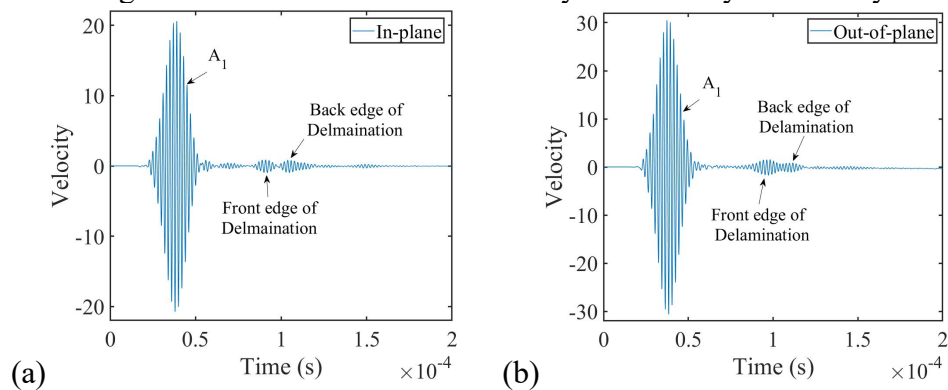


Fig.9 Waveforms for a HMC specimen with delamination at (70,7.2) mm from origin.

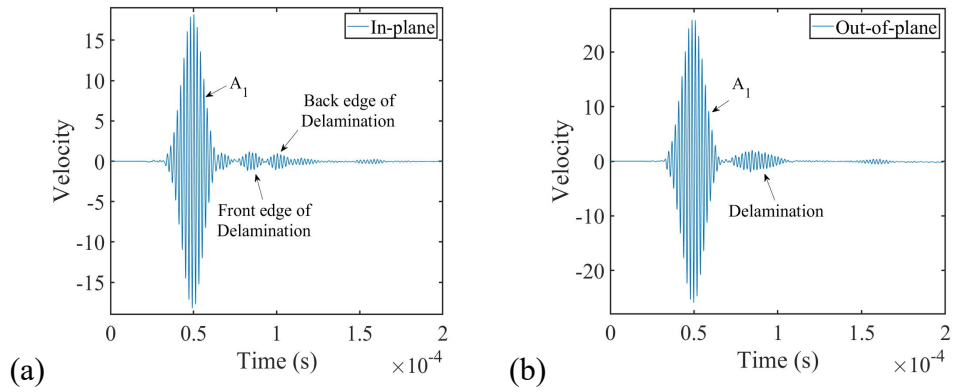


Fig.10 Waveforms for a HMC specimen with delamination at (100,7.2) mm from origin.

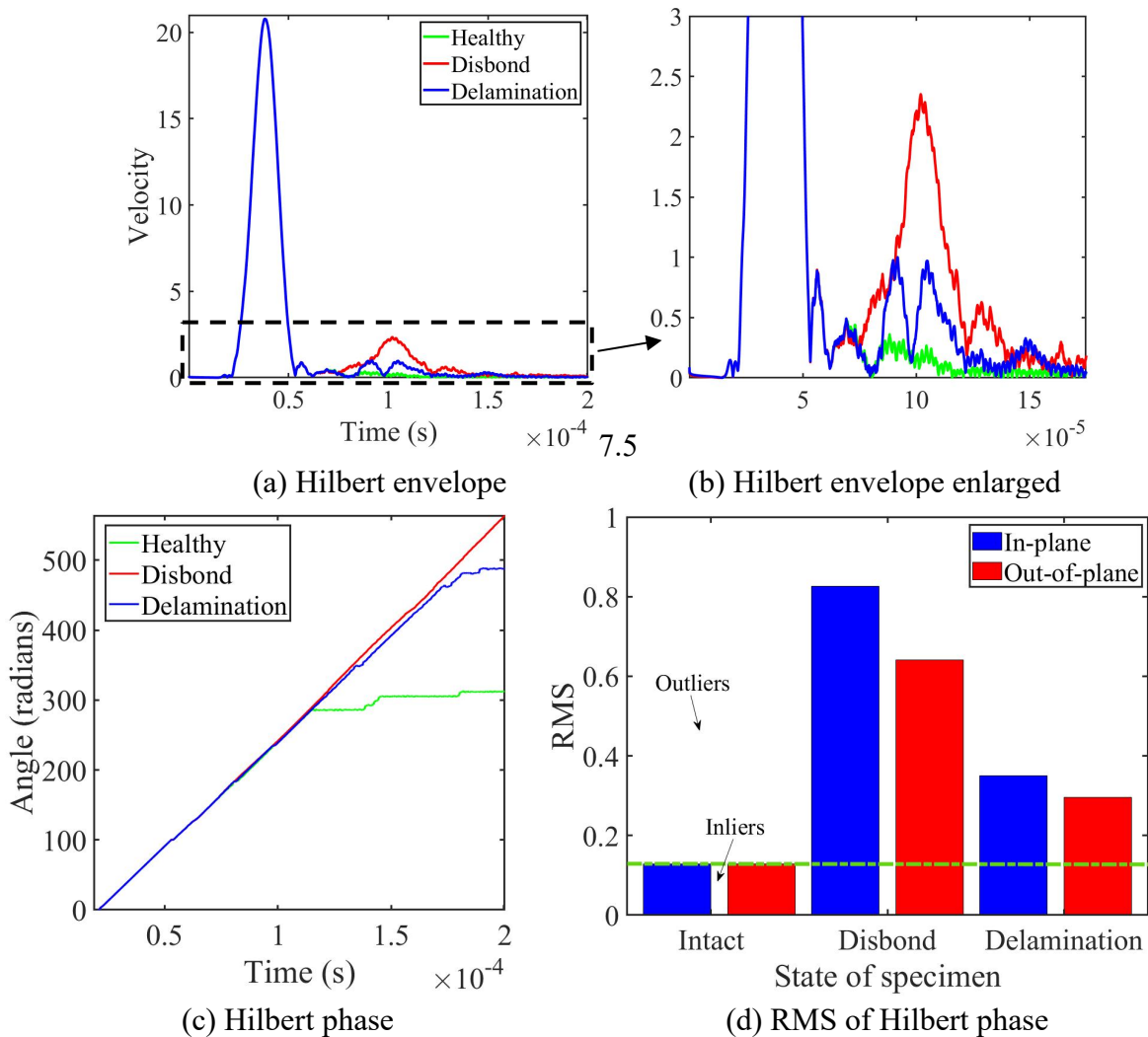


Fig.11 HHT for healthy and damaged HMC specimens (a) Hilbert envelope (b) Exaggerated image (c) Hilbert phase (d) Damage classification.

**Summary**

The present study focusses on the development of a damage diagnosis technique to detect different types of damages in a hybrid metal-composite (HMC) plate specimen using ultrasonic guided waves and outliers estimate. Dispersion curves of the HMC specimen were obtained to identify the most suitable frequency-mode pair for inspection. Based on the dispersion curves and wave

structure analysis,  $A_1$  Lamb mode at 500 kHz was found suitable to inspect the disbond and delamination damage in the HMC specimen. Wedge transducer was used to excite  $A_1$  Lamb mode into the specimen and time-domain responses were recorded at different propagation distances which were finally analyzed using HHT algorithm. Following are the concluding remarks from the present study:

1. The employed  $A_1$  Lamb mode was able to detect the disbond and delamination damage.
2. The Hilbert envelope not only helps localize the disbond and delamination damage but also evaluate its size along the wave propagation direction.
3. The Hilbert phase is used as a damage related feature to classify the detected damages in the HMC specimen.

### Acknowledgement

This work is supported by the Agency for Science, Technology and Research (A\*STAR), Singapore, under the RIE2020 AME Industry Alignment Fund - Prepositioning Programme (IAF-PP) (Grant number: A19C9a0044, A20F5a0043).

### References

- [1] V. Gonçalves, DM. Oliveira, AA. Santos, Comparison of ultrasonic methods for detecting defects in unidirectional composite material, *Materials Research*. 24 (2021). <https://doi.org/10.1590/1980-5373-mr-2021-0323>
- [2] FA. Masurkar, NP. Yelve, Optimizing location of damage within an enclosed area defined by an algorithm based on the Lamb wave response data, *Applied Acoustics*. 120 (2017) 98-110. <https://doi.org/10.1016/j.apacoust.2017.01.014>
- [3] YS. Andhale, F. Masurkar, N. Yelve, Localization of damages in plain and riveted aluminum specimens using Lamb waves, *International Journal of Acoustics & Vibration*. 24 (2019). <https://doi.org/10.20855/ijav.2019.24.11485>
- [4] Y. Lugovtsova, J. Bulling, C. Boller, J. Prager, Analysis of guided wave propagation in a multi-layered structure in view of structural health monitoring, *Applied Sciences*. 9(2019) 4600. <https://doi.org/10.3390/app9214600>
- [5] F. Yan, KX. Qi, JL. Rose, H. Weiland, Delamination defect detection using ultrasonic guided waves in advanced hybrid structural elements. *AIP Conference Proceedings*, 1211 (2010) 2044-2051. <https://doi.org/10.1063/1.3362372>
- [6] MR. Papanaboina, E. Jasiuniene, E. Žukauskas, L. Mažeika, Numerical analysis of guided waves to improve damage detection and localization in multilayered CFRP panel, *Materials*. 15 (2022) 3466. <https://doi.org/10.3390/ma15103466>
- [7] Z. Zhang, YF Ang, Ultrasonic defect inspection and characterization for wavy composites, 3<sup>rd</sup> Singapore international non-destructive testing conference and exhibition (2019).
- [8] M. Liu, F. Cui, Ultrasound defect detection in thick composites with out-of-plane waviness, 11<sup>th</sup> International symposium NDT in Aerospace (2019).
- [9] NE. Huang, SSP. Shen, The Hilbert-Huang transform and its applications, *Interdisciplinary mathematical sciences*, 5 (2005) 230- 244. <https://doi.org/10.1142/5862>
- [10] F. Masurkar, NP. Yelve, P. Tse, Nondestructive testing of rails using nonlinear Rayleigh waves. *Proceedings of the Institution of Mechanical Engineers, Part C: Journal of Mechanical Engineering Science* (2022). <https://doi.org/10.1177/09544062221086179>
- [11] NP. Yelve, F. Masurkar, P. Tse. Application of Rayleigh wave-based nonlinearity parameter to estimate the remnant useful life of fatigued thick aluminum plates. *ISSS Journal of Micro and Smart Systems*. 10 (2021) 161-78. <https://doi.org/10.1007/s41683-021-00074-5>